SCIENTIFIC CULTURE
www.sci-cult.com

SCIENTIFIC CULTURE, Vol. 12, No. 4, (2026), pp. 11674-11682
Open Access. Online & Print

DOI: 10.5281/zenodo.124261107

EARLY DETECTION OF SPINAL CORD GLIOMAS USING U-NET++ SEGMENTATION AND XGBOOST-BASED CLASSIFICATION ON MRI IMAGES

Dr G Shyama Chandra Prasad[1]*, Sowmya Dondeti[2], Dr. J Srinivas[3], Dr Para Rajesh[4], Dr Amaravrapu Pramod Kumar[5]

[1]Professor of CSE and Principal, Bhoj Reddy Engineering College for Women, Saidabad, Hyderabad, Email: gscprasad@gmail.com, ORCID: 0000-0001-9223-3060.
[2]Assistant Professor, CSE-AIML, VNR Vignana Jyothi Institute of Engineering and Technology,Vignana Jyothi Nagar, Pragathi Nagar, Nizampet, Hyderabad, Telangana - 500118, Email: chowdarymadhu65@gmail.com, ORCID: 0009-0002-6100-6900
[3]Associate Professor, Dept. of Information Technology, Matrusri Engineering College, Saidabad, Hyderabad, Email: jagirdar.srinivas@gmail.com, ORCID: 0000-0002-3639-1627
[4]Assistant Professor, Computer Science and Engineering,VNR Vignana Jyothi Institute of Engineering and Technology,Hyderabad,Telangana-500090,India, Email: pprr21@gmail.com, ORCID: 0000-0001-9056-5918
[5]Assistant Professor, CSE- (CyS ,DS) and AI&DS, VNR Vignana Jyothi Institute of Engineering and Technology, Hyderabad,Telangana-500090,India, Email:amaravarapupramod@gmail.com, ORCID: 0000-0001-5861-8960

Received: 22/11/2025
Accepted: 08/02/2026

Corresponding Author: Dr G Shyama Chandra Prasad (gscprasad@gmail.com)

ABSTRACT

The most prevalent primary brain tumors are gliomas. I am going through a divorce. According to the World Health Organization's (WHO) recommendations, there are four classes (classes I–II–III–IV). The accurate grading of gliomas is essential for pre-diagnosis, monitoring, chemotherapy administration, and prognosis treatment planning. This study uses deep learning architectures for segmentation and classification to provide a novel approach for the early diagnosis of spinal cord gliomas. In this case, the input image has undergone pre-processing to eliminate noise, resize, and smoothing image. U-Net++ architecture used to segment the processed image, were as XG_Boost architecture was used to classify sections of the skull or vertebral column. A publicly available MR image dataset of 3065 from 233 patients, the performance of our method is compared against previously published deep learning and machine learning techniques. The classification of tumor with accuracy of 96.8 percentage, our approach considerably beat the other approaches using the identical datasets in the comparison.

KEYWORDS: Deep Learning, Segmentation, Classification, Gliomas, Brain Tumors.

Copyright: © 2026. This is an open-access article distributed under the terms of the Creative Commons Attribution License. (https://cre-ativecommons.org/licenses/by/4.0/).

OVERVIEW

Gliomas are primary malignant tumors with a high death and recurrence rate that often arise in the brain. According to Cancer Society of America , In 2018, 23,880 patients were diagnosed with malignant brain and spinal cord tumors; of these, 70% passed away [1]. Grades I through IV are commonly used to classify gliomas. As per WHO classifies gliomas according to their level of malignancy, ranging from Grade II (lower grade) to Grade IV (high grade) [2]. Among the most prevalent brain malignancies are meningiomas, gliomas, and hypoyphosis tumors [3]. Low-grade gliomas, diffuse Grade-II and Grade-III gliomas, and tumors with highly variable behaviours and textural with unpredictable features are all included by the World Health Organization. Furthermore, the WHO defines low-grade gliomas as infiltrative neoplasms that typically contain medium-grade and low-grade gliomas (Grade II and Grade III) [4]. Grade II and Grade III brain tumors include oligodendrioglioma, oligoastrocytoma, and astrocytoma. Examining brain tumor types in the relevant classes may help treat brain cancers, as these tumors fall into the Grade-II or Grade-III groupings.

There are two types of astrocytomas: Grade II (i.e. low grade) and Grade III (i.e. high grade). In certain regions, low-grade astrocytomas grow slowly.

Different treatment approaches are needed for high-grade astrocytomas because they grow quickly [5]. These cells don't resemble normal cells at all, and Grade II tumors have malignant tissues. Grade III tumors are defined as aggressively proliferating malignant tissue cells. It is very difficult and demanding clinically to provide low and medium grade cancers employing cellular and MRI imaging. Brain tumor detection, growth prediction, and treatment can all benefit from automatic medical image segmentation and classification. Because detection of early brain tumors implies a quick response to treatment, it increases patient survival rates. Search and categorize brain tumors I large medical image databases by contribution along the method routine clinical duties is necessary a significant amount of time and effort. An automated approach to detection, localization, and categorization is beneficial. Numerous medical imaging modalities Used to get the kind, Shape, size, location, etc other information is necessary for tumor detection[5].

Among the most significant methods are computed tomography (CT), magnetic resonance spectroscopy (MRS), positron emission tomography (PET), magnetic resonance imaging (MRI), and single photon emission computed tomography (SPECT). Several techniques could be combined to get more precise information about the tumor. In any case, MRI is the most often utilized method because of its benefits. In an MRI, hundreds of 2D picture slices with strong soft tissue contrast are created without the use of ionization radiation. The T1 weight is used in the four MRI modes for diagnosis MRI (T1), T2 weighted MRI (T2), and enhanced T1-weighted contrast. Fluid Attenuated Inversion Recovery (FLAIR) with MRI (T1-CE).since they create images. MRI contrasts between different tissues It is better to determine how one kind of tissue differs from another. When interacting with healthy tissues, the T1 modality is frequently employed.[6].

RELATED TASKS

Recently, machine learning (ML) and deep learning (DL) approaches have become popular. Brain tumor detection and categorization using several imaging modalities, particularly those made possible by MRI. The most current and relevant studies on the subject of the paper appear in this part. Work [7] proposes a system that blends discrete wavelet transform (DWT) characteristics with deep learning (DL) techniques. Following division, the brain tumor Go DWT was utilized to extract functions for every lesion that was discovered utilizing the fuzzy c-mean approach. These features were reduced in dimension using principal component analysis (PCA), and the chosen features were then fed into deep neural networks (DNN). They achieve a 96.95% accuracy rate and a 97.01% sensitivity.

The Gray Level Co-occurrence Matrix (GLCM) and convolutional neural networks (CNNs) were used in a brain tumor classification technique described in characteristics based on 8. They did. The exam. Using four different datasets (Mg-Gl, Mg-Pt, Gl-Pt, and Mg-Gl-Pt), they found that the Gl-Pt dataset had the best accuracy (82.27%). Using contrast and uniformity as two sets of characteristics employing correlation.

From four angles (0°, 45°, 90°, and 135°), they extracted four properties from each image: energy, correlation, contrast, and homogeneity. The author proposed an automated brain tumor diagnosis and grading approach based on CNN. By applying the technique FCM, or fuzzy C-means To the section From the perspective of these common places,

Features of shape and structure are gathered and fed. DNN and SVM classifiers. The results showed that the system was accurate. 97.6%.

However, function [10] used precision ring-form distribution and ROI augmentation to improve the effectiveness of the brain tumor classification procedure.

These enhancements are used in a number of feature extraction methods, such as the bag-of-words (BoW), GLCM, and intensity histogram, where various feature vectors are supplied in a hierarchy. The accuracy for intensity histogram, GLCM, and BoW improved from 71.39% to 78.18%, 83.54% to 87.54%, and 89.72% to 91.28%, respectively, according to the experimental findings. In order to decrease the feature dimension of the wavelet feature set, a genetic algorithm feature selection was suggested [11]. Perspective is based on choice. The ideal feature vector is supplied into the chosen classifier, such as an artificial neural network (ANN). The findings demonstrate that the genetic algorithm just made the decision. Only four of the 29 features were available, and their correctness was 98%.

The author of [12] proposed a method For non-aggressive classification brain tumors glioma by using an altered AlexNet CNN. Whole- brain MRI scans was used for the classification process, and was attached to the label. The image level instead of the pixel level. Combined with a comprehensive strategy for data amplification CNN to brain tumor classification I was proposed. Work [13] and With an accuracy of 91.16%, the trial results showed that the method worked fairly well.

This method used user segmentation. MRI pictures of brain tumors Brain tumors are categorized into several grades. They understood. An overall accuracy of 87.38% And 90.67% Employment A pretrained VGG-19 CNN architecture was used for transferee learning classification both before and after the influx in data..

I contribute to the classification of brain cancers [14]. A particular entropy is applied to the CNN using neutrosophic expert maximal fuzzy (NS-CNN). CNN uses these images as input for feature extraction after the distribution of brain tumors using the neutrosophic set-expert maximal fuzzy-sure algorithm. and then fed SVM classifiers Too benign or malignant categorization.

They have a success rate of 95.62%. In order To diagnose correctly a range of cancer subtypes, They developed a crossover method for a novel cuckoo search [15]. Benchmarks were used to evaluate cancer gene expression. The model, And the results illustrate. CSC performed better than CS And other established techniques. I used the auxiliary method. [16] for dimension reduction and functional classification.

Convolutional neural networks (CNN) and support vector machines (SVM) were the most commonly employed methods for prediction [17]. The experiment's results Consider the recommended approach. may improve CNN and SVM classification methods' accuracy. Lastly, in order to enhance the efficiency of gene selection in microarray data, A novel multivariate characteristic was suggested by the author [18]. Method of classification.

MATERIALS AND TECHNIQUES

To partition tumors and create a classification system, we used a U-Net++ architectural network. Using the XG_Boost architecture as a basis. In order to segment and classify the training dataset, we first employed a single U-Net++. Every image in the collection is in grayscale, with the foreground in the middle. The size and location of the tumors fluctuate depending on the angle from which the images are taken of the skull. The tumor diagnosis is challenging because of these variations in tumor size. In reality, the skilled doctor is aware of the direction in which the MR image was taken. We chose to replicate the identical situation for deep neural networks since their learning process is comparable to that of humans. We found that employing a single network to identify cancers in every image is wrong. Figure 1 depicts the overall suggested architecture.

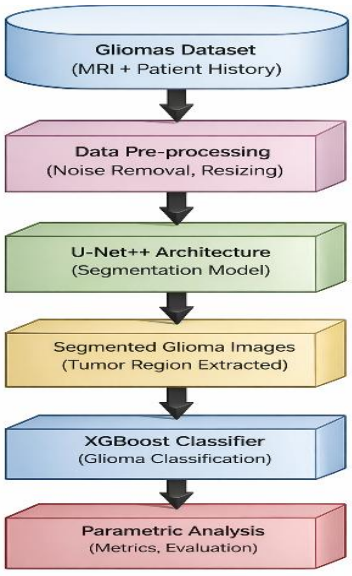

Figure 1: Overall proposed Architecture

Preparing the data and describing the dataset

In clinical settings, only a small number of brain CE-MRI discs with a wide disc gap rather than a 3D volume are regularly obtained and made available. The difficulty lies in creating a 3D model with very little informationConsequently, 2D is the foundation of the suggested approach. Between 2005 and 2010, the disks were gathered from 233 patients at Tianjing Guangzhou, China's Nanfang Hospital and Medical University's General Hospital.

Sagittal, coronal, and axial images of pituitary tumors (930), gliomas (1426), and meningiomas (708). This dataset contains 3064 Cutting**.**

Examples Of these three tumor forms appear in Figure 1. This dataset also has five-fold cross-validation indices. In order to use this data, 80% (2452) 20% (612 images) of the pictures used for training used to assess performance. The process is completed five times. Images have. 0.49 x 0.49 mm2 pixels with a 512 x 512 pixel in-plane resolution. The participant has a 1 mm difference and a thickness of 6 mm. Three proficient radiologists meticulously sketched the margins of the tumor.

The patient's pid is contained in an information structure that is connected to each image in the dataset. The coordinate vector (x, y) of the spots that make up the tumor boundary is the tumor type label (lgt), which is 1 for meningioma, 2 for glioma, and 3 for glioma. pituitary tumor; and tumor mask (Tij), a binary image that has a value of 1 for tumor locations and 0 for healthy areas will make use of the training procedure. The ground reality is the pair lgt, Tij Seam.

Data augmentation via an elastic transform has been used to prevent the neural network from overfitting during training. With each fold iteration, go data augmentation the process is two- fold the number of training images accessible, to now 4904 Pictures from everyone image in the training dataset, An extensive procedure was followed for extraction. 65 x 65 pixel training examples: 150 real-world instances of positive windows Additionally, There are 325 real negative window examples for every tumor. Pixel standardization (zero mean and unit variance) was used for scaling. The training dataset's pixels but these windows.

Gliomas segmentation with U-Net++

The shallow and deep layers of the prior baseline design did not exchange contextual information. A module that can serve as an information bridge between shallow and deep levels must be included in order to enhance the network's local and global characteristics. The planned BU-Net's general layout, which includes a WC block and RES blocks, is depicted in Figure 2. After receiving input photos with a resolution of 256 × 256, the architecture produces images with identical dimensions. The left and right portions of the model serve as encoders and decoders, respectively. U-Net++ uses convolution layers with padding. This enables the output image to be the same size as the input image. The network's encoder and decoder are separated into blocks. Each encoder side block consists of two convolution layers, one max-pooling layer, and one dropout layer. The Conv2DTranspose layer is applied to the output of the preceding block at the beginning of each decoder side block. The output from the corresponding RES block is concatenated with the output of the Conv2DTranspose layer. Two convolution layers are applied to the concatenated output following dropout. Another convolution layer with six 1 × 1 filters is found in the decoder's last block. The image is contracted by the encoder side and expanded by the decoder side.

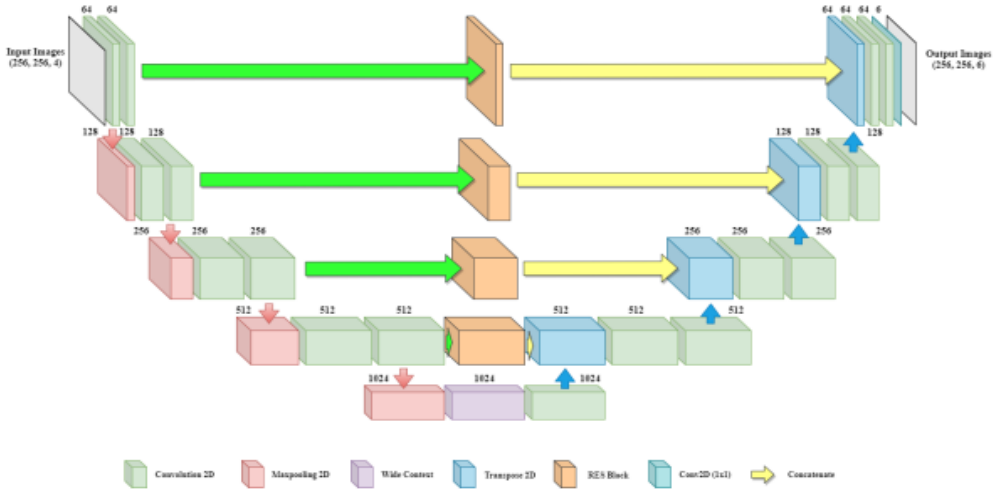

Figure 2: The suggested U-Net++ design for glioma segmentation

Furthermore, The architecture uses a big context block to transition from the encoder to the decoder. With the exception of the last convolution layer, which employs a sigmoid activation function, each convolution layer in U-Net++ is followed by batch normalization and the ReLU activation function. The following are the numerical representations of the sigmoid activation function and ReLU:

$$\text{ReLU}\,(q) = \begin{cases} 0, & \text{if } q \le 0 \\ q, & \text{otherwise} \end{cases}$$

$$\text{Sigmoid}\,(q) = \frac{1}{1 + \exp\,(-q)}$$

U-Net++ is implemented using the Keras framework. [37]. After a range of dropout rates were examined using hyper-parameter tuning, the network's optimal dropout ratio was determined to be 0.3. The updated loss function was combined with the Adam optimizer. With a momentum of 0.9, the learning rate was set at 0.01. A batch size of 16 and early halting based on validation loss with a patience level of 10 yielded the highest number of training iterations. Five parallel connections are used by the architecture to receive the input. Two convolutional layers are used in the first four. We have employed a filter size of N × 1 for the first convolution layer and 1 × N for the second convolution layer for every link with convolution layers. We used two cascaded convolution layers rather than a single convolution layer with a N × N filter size. Using two convolution layers results in fewer parameters, which enhances the architecture as a whole. Additionally, Testing showed that the effect of a single convolution layer with more parameters is comparable to that of cascaded convolution layers with fewer parameters. The input is received exactly as it was forwarded by the last connection, a skip connection. The outputs from five connections are added to create one output. Three successive convolution layers are applied to the summed output. The filter sizes of the three convolution layers are 3 × 3, 3 × 3, and 1 × 1. To stop information degradation, the RES block transforms low-level attributes into middle-level features. The residual extended skip is scale-invariant because it executes contextual aggregation on several dimensions for the incredibly diverse cancer locations. Better segmentation is made possible by the RES, which expands the valid receptive field.

Two parallel connections receive the input to WC. There are two convolution layers in each link. The two convolution layers in the first connection use N × 1 and 1 × N, respectively. The filter size of the second connection is 1 × N, and the filter size of the convolution layer that follows is N × 1. These two links work together to create a helpful feature set that can improve performance. It was found that both combinations can have an impact on the outcome and that a change in combination alters the retrieved features. An output of WC is produced by adding the outputs from both connections.The broad context (WC), like RES, collects contextual information necessary to distinguish between various cancer subtypes. Additionally, by combining data at the transition level, it enhances the segmented sections' reconstruction.

98.46% of the area in an MRI of a brain tumor is composed of healthy tissues. The augmenting tumor region takes up 29.01% of the brain tumor MRI image, whereas 1.02% is occupied by the edema area. Just 23.00% of the space is occupied by the non-enhancing tumor. The performance of segmentation is negatively impacted by the large disparity. The loss function has two objective functions: weight cross-entropy (WCE) is used to classify the tissue cells based on their class, and dice loss coefficient (DLC) is used to determine the largest overlap between the ground truth and predicted segmented regions regardless of class.

Classification of Gliomas using XG-Boost:

An effective gradient-boosted decision tree technique is called XGBoost. A method known as gradient boosting was proposed by XGB. Once the new models have been fitted to residuals from previous models, gradient descent is used to minimize the combined results. Tumors can be classified using a variety of characteristics, and an efficient medical diagnostic system can be created by extracting a variety of features based on the type of data. We could identify if a tumor is malignant or benign or we could categorize brain imaging and tumors as normal, aberrant, and neutral. Our work focuses on the latter, and a dataset of over fifty photos is used to generate results.Both supervised and unsupervised learning models are commonly used to determine the best classifier. Improvements and hybrid methods are being created and evaluated for the same. Extreme Gradients Boost Decision-Making While Decision-Making and Random Forests An intriguing viewpoint is provided by trees, which have recently been shown to be a reliable replacement for every other learning model. We use XGBoost, an extreme gradient boost program, to implement it. Extreme Gradient Boosted Machines (EGBM) is a supervised learning model that combines weak learners or classifiers to produce a powerful classifier. Unlike Random

Forests (RF), which employ learners with low biases but large variance, weak learners have high biases and low variances. Because humans can observe how and why computers make decisions, they are superior to neural nets. Let's say we have two classifier trees or weak learners, each of which demonstrates a distinct but erroneous part of the issue. In XGBoost, we go through iterative phases where we employ weak classifiers to build on top of one another so that we have the best step at each level, whereas in RF, we continue to build the trees in parallel. We optimize each step because each weak learner now builds upon the preceding tree instead of working individually. Thus, if we have one tree with two conditions (C1, C2) (Fig. 8. (a)) and another tree with condition C3, the boosted value is the sum of both weak learners, A=2+.5, and so on. When we prune the final tree in a bottom-up parsing, the user is also aware of the depth because the full tree has been constructed. These ensemble tree approaches with sequential structure and iterative improvements have shown faster and more accurate results than traditional GBMs by employing 5-fold cross-validation for verification [14, 15]. We cross-validated the data and used 50 photos to classify brain tumors with 100% accuracy. The computation was finished quickly, and the findings were in line with our expectations.

The idea is to grow a tree by separating features and adding new trees on a regular basis.

$$\hat{y}_i = \phi(x_i) = \sum_{k=1}^{T} f_k(x_i), f_k \in \mathcal{F}$$

The function is defined as:

$$\mathcal{F} = \{f(x) = w_{q(x)}\}(q: R^m \to T, w \in R^T)$$

Where y_i is the projected label of the i^{th} sample, Each tree's structure, q, associates each example with its matching leaf index, f_k is the kth tree model, and the total number of trees as T. The goal function of the XGBoost classifier is defined as follows.

$$L(\phi) = \sum_{i=1}^{n} l(\hat{y}_i, y_i) + \sum_{k=1} \Omega(f_k), \text{ where } \Omega(f) = \gamma$$

The objective function consists of two terms. The loss function, which measures the discrepancy between the expected and actual values, is the first term. The regularization term is the second term. T and w stand for the number and weight of leaf nodes, respectively. γ determines the number of leaf nodes, while λ prevents overfitting. It automatically learns a new function to suit the residuals from the previous forecast each time a tree is added. The expected value of the sample must be calculated by adding the scores of each tree if we have k trees after training. We employ the XGBoost classifier as the model with a maximum depth of nine, learning rate γ of 0.1, and λ of 0.3 for the study's numerical experiments using 10-fold cross-validation.

Examining E-experiments

The results of the numerous tests carried out to evaluate the performance of the suggested hybrid model are shown in this section. The suggested hybrid model was tested using a PC equipped with the following features: In addition to the Python 2.7 programming language and the NumPy, SciPy, Pandas, Keras, and Matplotlib frameworks, the Intel(R) Core (TM) i5-7500 CPU boasts a 32-bit operating system, 4 GB of RAM, and Windows 7.

We examined the genetic profiles of 28 patient samples (data set A: supratentorial PNETs, renal and extrarenal rhabdoid tumors, medulloblastomas, CNS AT/RTs, and normal human cerebella). The suggested hybrid model's performance was assessed using eight-fold cross-validation in our experiments, and the results are shown as an average standard deviation. Each test was also conducted thirty times. F-1 Score, Accuracy, Precision, and Recall were the evaluation techniques employed in our trials.

The estimation of True Positive (TP), False Negative (FN), True Negative (TN), and False Positive (FP) are used to assess the parameters.

The ratio of correctly predicted values to all forecasts was used to define accuracy. The accuracy is defined as (TP+TN)/(TP+TN+FP+FN).

Recall or sensitivity is defined as the ratio of the correctly predicted value to the total forecast value. The definition is Recall=((TP)/(TP+FN)).

Precision: All positive actual values are divided by all expected values. Precision is equal to (TP/(TP+FP)).

The average precision to recall ratio is provided by the F1-Score. This is how the F1-Score is calculated: F1-Score = 2 * (Precision * Recall)/(Precision + Recall)

Table 1: A comparison of the suggested and current methods

Characteristics (%)	CNN	KNN	SVM	DNN	U-net with VGG-19	U-net++ with XGboost (propose)
Accuracy	88.0	89.0	91.0	93.0	93.52	96.8
Precision	86.0	85.0	84.0	94.2	93.4	96.96
Recall	77.0	75.0	76.0	87.6	92.42	96.26
F1 - Score	79.0	80.0	81.0	80.0	92.0	96.57

A comparison of the suggested and current methods for detecting gliomas based on segmentation and classification approaches is presented in Table 1 above. CNN, KNN, SVM, DNN, and U-net_VGG-19 have been compared with the suggested method. Below are the comparison graphs.

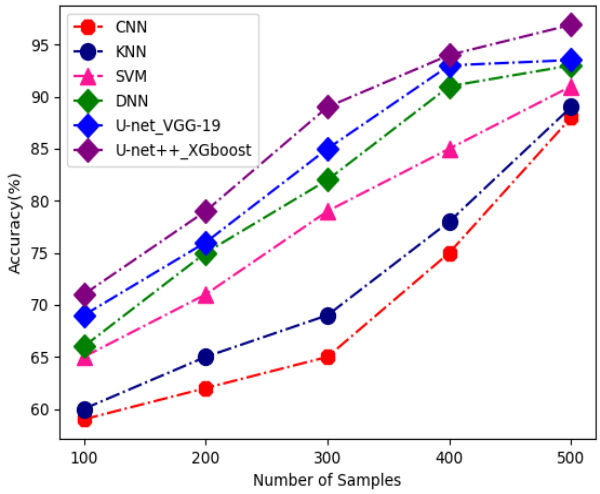

Figure-3 A comparative evaluation of accuracy

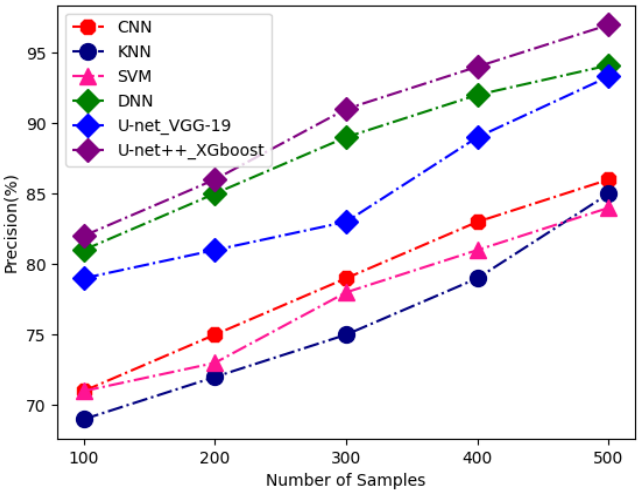

Figure 4: Accurate Comparative Evaluation

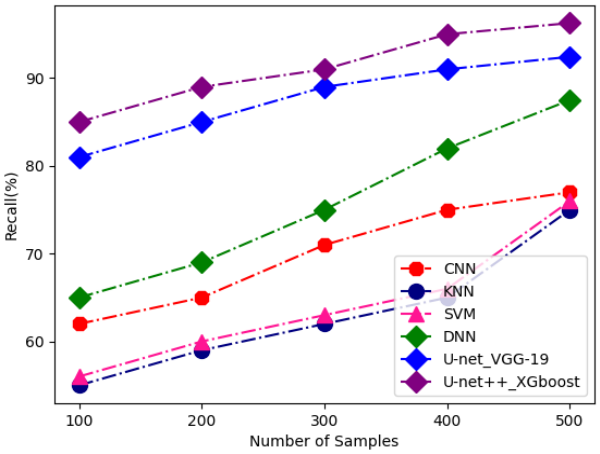

Figure 5: Recall Comparative Evaluation

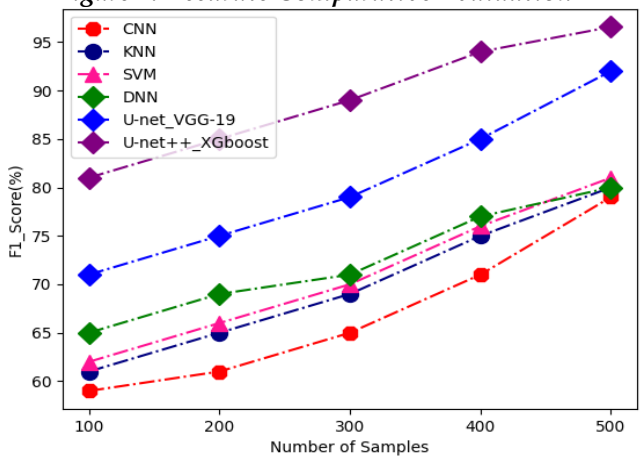

Figure 6: Comparison of F-1 scores

The comparison study based on suggested and current glioma detection methods is depicted in Figure 2-5 above. In this case, the suggested method produced the best outcomes Regarding memory, precision, accuracy, and F-1 score. In comparison to the current approach, the suggested methodology U-net++_XGboost obtained 96.9% accuracy, 96.97% precision, 96.27% recall, and 96.56% F-1 score. The accuracy of the tumor's detection is improved with less processing time. Figure 6 displays the entire comparison.

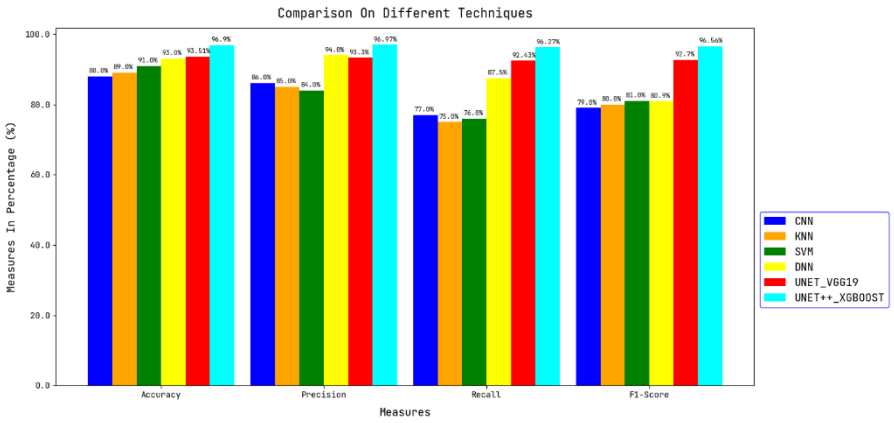

Figure 7: Overall parametric comparison for glioma detection

In conclusion

This study suggested a unique method for early glioma identification using segmentation and classification based on deep learning. Here, we used a publically accessible dataset of T1-weighted contrast-enhanced MRI scans to assess its performance. Data augmentation by elastic Transformation was employed to increase the training dataset and prevent overfitting. We have developed a novel model with an improved encoder-decoder architecture for the precise segmentation of brain tumors. We have extended the U-Net++ architecture with two new blocks: wide context (WC) and residual extended skip (RES). The XG_Boost based classifier frequently adds parameters to the cost function, such as the number of leaf nodes in the tree and the score sum of squares on each leaf node, to manage the model's complexity. The regular term simplifies the trained classifier and lowers the variation of the classifier from the standpoint of bias variance. As a result, it outperforms the other four classifiers and is more effective at preventing overfitting during training. The results may be useful in determining the machine learning model and understanding abnormal situations in the actual world. According to the BRATS 2013 benchmark, the obtained performance metrics rank in the top 10. We compared our results with seven different techniques that use the same data to categorize brain tumors. Our approach offers the highest scoring and tumor classification accuracy 96.8%.

REFERENCES

1. Siegel, R.L.; Miller, K.D.; Jemal, A. Cancer statistics, 2021. CA A Cancer J. Clin. 2021, 66, 7–30.
2. Rehman, M.U.; Cho, S.; Kim, J.; Chong, K.T. BrainSeg-Net: Brain Tumor MR Image Segmentation via Enhanced Encoder–Decoder Network. Diagnostics 2021, 11, 169.
3. Isensee, F.; Jäger, P.F.; Full, P.M.; Vollmuth, P.; Maier-Hein, K.H. nnU-net for brain tumor segmentation. In International MICCAI Brainlesion Workshop; Springer: Cham, Switzerland, 2020; pp. 118–132.
4. Zeineldin, R.A.; Karar, M.E.; Coburger, J.; Wirtz, C.R.; Burgert, O. DeepSeg: Deep neural network framework for automatic brain tumor segmentation using magnetic resonance FLAIR images. Int. J. Comput. Assist. Radiol. Surg. 2020, 15, 909–920
5. Perrin, S.L.; Samuel, M.S.; Koszyca, B.; Brown, M.P.; Ebert, L.M.; Oksdath, M.; Gomez, G.A. Glioblastoma heterogeneity and the tumour microenvironment: Implications for preclinical research and development of new treatments. Biochem. Soc. Trans. 2019, 47, 625–638.
6. Rehman, M.U.; Cho, S.; Kim, J.H.; Chong, K.T. BU-Net: Brain Tumor Segmentation Using Modified U-Net Architecture. Electronics 2020, 9, 2203.
7. Pei, L.; Vidyaratne, L.; Rahman, M.; Iftekharuddin, K.M. Context aware deep learning for brain tumor segmentation, subtype classification, and survival prediction using radiology images. Sci. Rep. 2020, 10, 1–11.
8. Pradana, A.C.; Aditsania, A. Implementing binary particle swarm optimization and C4.5 decision tree for cancer detection based on microarray data classification. J. Physics: Conf. Ser. 2019, 1192, 012014.
9. Shukla, A.K.; Tripathi, D. Detecting biomarkers from microarray data using distributed correlation based gene selection. Genes Genom. 2020, 42, 449–465.
10. Sampathkumar, A.; Rastogi, R.; Arukonda, S.; Shankar, A.; Kautish, S.; Sivaram, M. An efficient hybrid methodology for detection of cancer-causing gene using CSC for micro array data. J. Ambient. Intell. Humaniz. Comput. 2020, 11, 4743–4751.
11. Kilicarslan, S.; Adem, K.; Celik, M. Diagnosis and classification of cancer using hybrid model based on ReliefF and convolutional neural network. Med. Hypotheses 2020, 137, 109577.
12. Naser, M.A.; Deen, M.J. Brain tumor segmentation and grading of lower-grade glioma using deep learning in MRI images. Comput. Biol. Med. 2020, 121, 103758.
13. Lee, J.; Choi, I.Y.; Jun, C.-H. An efficient multivariate feature ranking method for gene selection in high-dimensional microarray data. Expert Syst. Appl. 2021, 166, 113971.
14. Sukumaran, A., & Abraham, A. (2022). Automated Detection and Classification of Meningioma Tumor from MR Images Using Sea Lion Optimization and Deep Learning Models. *Axioms*, *11*(1), 15.
15. Karayegen, G., &Aksahin, M. F. (2021). Brain tumor prediction on MR images with semantic segmentation by using deep learning network and 3D imaging of tumor region. *Biomedical Signal Processing and Control*, *66*, 102458.
16. Krishna, N., Khalander, M. R., Shetty, N., &BharathBhushan, S. N. (2021). Segmentation and detection of glioma using deep learning. In *Advances in Artificial Intelligence and Data Engineering* (pp. 109-120).

Springer, Singapore.
17. Díaz-Pernas, F. J., Martínez-Zarzuela, M., Antón-Rodríguez, M., & González-Ortega, D. (2021, February). A deep learning approach for brain tumor classification and segmentation using a multiscale convolutional neural network. In *Healthcare* (Vol. 9, No. 2, p. 153). Multidisciplinary Digital Publishing Institute.
18. Gurunathan, A., & Krishnan, B. (2021). Detection and diagnosis of brain tumors using deep learning convolutional neural networks. *International Journal of Imaging Systems and Technology*, *31*(3), 1174-1184.